EPR Studies on a Stable Sulfinyl Radical Observed in the Iron−Oxygen-Reconstituted Y177F/I263C Protein R2 Double Mutant of Ribonucleotide Reductase from Mouse†

Annie Adrait,‡,§ Maria Öhrström,‡,§ Anne-Laure Barra,|| Lars Thelander,⊥ and Astrid Gräslund*,§

Department of Biochemistry and Biophysics, The Arrhenius Laboratories for Natural Sciences, Stockholm University, SE-106 91 Stockholm, Sweden, The High Magnetic Field Laboratory, CNRS/MPI, F-38042 Grenoble Cedex, France, and Department of Medical Biochemistry and Biophysics, Umeå University, SE−901 87 Umeå, Sweden

Received November 12, 2001; Revised Manuscript Received March 25, 2002

ABSTRACT: Ribonucleotide reductase (RNR) catalyzes the biosynthesis of deoxyribonucleotides. The active enzyme contains a diiron center and a tyrosyl free radical required for enzyme activity. The radical is located at Y177 in the R2 protein of mouse RNR. The radical is formed concomitantly with the μ-oxo-bridged diferric center in a reconstitution reaction between ferrous iron and molecular oxygen in the protein. EPR at 9.6 and 285 GHz was used to investigate the reconstitution reaction in the double-mutant Y177F/I263C of mouse protein R2. The aim was to produce a protein-linked radical derived from the Cys residue in the mutant protein to investigate its formation and characteristics. The mutation Y177F hinders normal radical formation at Y177, and the I263C mutation places a Cys residue at the same distance from the iron center as Y177 in the native protein. In the reconstitution reaction, we observed small amounts of a transient radical with a probable assignment to a peroxy radical, followed by a stable sulfinyl radical, most likely located on C263. The unusual radical stability may be explained by the hydrophobic surroundings of C263, which resemble the hydrophobic pocket surrounding Y177 in native protein R2. The observation of a sulfinyl radical in RNR strengthens the relationship between RNR and another free radical enzyme, pyruvate formate-lyase, where a similar relatively stable sulfinyl radical has been observed in a mutant. Sulfinyl radicals may possibly be considered as stabilized forms of very short-lived thiyl radicals, proposed to be important intermediates in the radical chemistry of RNR.

The enzyme ribonucleotide reductase (RNR)[1] catalyzes the reduction of all four ribonucleotides to the corresponding deoxyribonucleotides, a reaction necessary for DNA replication (*1*−*4*). A number of enzymes from different organisms have been described and classified into three major classes (*1*). The class I enzymes, which are the most studied, are found in mammals, plants, DNA viruses, and some prokaryotes such as *Escherichia coli*. They are composed of two nonidentical homodimeric components, proteins R1 and R2 (*5, 6*).

The three-dimensional structures of proteins R1 and R2 from *E. coli* and that of protein R2 from mouse have been determined separately, and the holoenzyme from *E. coli* has been model-built (*7*−*9*). Despite the low sequence homology between mouse and *E. coli* R2 (10), the overall structure and the important enzymatic features are very similar (*11*). The specific substrate reaction takes place in the larger R1 component, whereas the free radical on a tyrosyl side chain (Tyr^{122} in *E. coli* and Tyr^{177} in mouse) required for enzymatic activity is generated in the smaller R2 component (*1, 5, 6*). The tyrosyl radical is deeply buried in the interior of the mouse and *E. coli* R2 proteins. This excludes direct interactions with the substrate at the active site on R1, and a long-range electron-transfer pathway of conserved hydrogen bonded amino acids connects the substrate binding site in R1 to the radical-harboring tyrosyl residue in R2 (*7, 8*). The electron-transfer pathway includes the conserved amino acids (Fe1) His^{173}-Asp^{266}-Trp^{103}-Tyr^{370} in R2 and Tyr^{738}-Tyr^{737}-Cys^{429} in R1 (mouse numbering). The enzyme loses activity when this pathway is disturbed by mutations (*12*−*14*). It has also been shown that the radical transfer pathway in mouse protein R2 is involved in the generation of the tyrosyl radical (*15*).

The tyrosyl radical in R2 is generated by abstraction of an electron from the tyrosine residue (Tyr^{122} in *E. coli* and Tyr^{177} in mouse) during oxidation of two ferrous ions bound in the vicinity of the tyrosine. This reconstitution reaction, which is driven by molecular oxygen, also generates the μ-oxo-bridged diferric iron center of R2. Many studies of the iron reconstitution reaction have been performed, but all details of the mechanism for oxygen activation and radical formation are not yet clarified.

† This work was supported by grants from the Swedish Research Council, the Swedish Foundation for Strategic Research, and the European TMR program under contract No. ERBFMRXCT89027.

* To whom correspondence should be addressed. E-mail: astrid@dbb.su.se. Phone: +46-8-162450. Fax: +46-8-155597.

‡ Both are to be considered first authors.

§ Stockholm University.

|| The High Magnetic Field Laboratory.

⊥ Umeå University.

[1] Abbreviations: RNR, ribonucleotide reductase; RFQ, rapid freeze quench; SFQ, slow freeze quench.

10.1021/bi012043d CCC: $22.00
Published on Web 04/26/2002

The tyrosyl radical in protein R2 has a unique stability not yet fully understood. One stabilizing factor has been proposed to be the diferric center, to which the radical is magnetically coupled (*16*). Another factor that has been proposed is the hydrophobic pocket surrounding the radical site. Site-directed mutagenesis of the pocket in *E.coli* R2 has shown that changing only one hydrophobic amino acid for a hydrophilic one leads to a drop in the lifetime of the radical by several orders of magnitude (*17*). The pocket is composed of three conserved hydrophobic residues, Phe^{208}-Phe^{212}-Ile^{234} in *E.coli* and Phe^{237}-Phe^{241}-Ile^{263} in mouse R2. The isoleucine residue is in van der Waals contact with the side chain that produces the tyrosyl radical (*7, 11*).

In a previous study to investigate if other oxidizable amino acids positioned at the site of the radical-harboring tyrosyl residue could harbor free radicals and initiate catalysis, Tyr^{177} from mouse R2 was mutated to either tryptophan or cysteine (*18*). In the same study, a mutant where Tyr^{177} was replaced by the nonoxidizable amino acid phenylalanine was constructed. The phenylalanine replacement was done in order to look for side pathways or suppressed radicals, as previously observed in the corresponding *E. coli* protein R2 mutant, e.g., Tyr^{122} to phenylalanine (*19, 20*). The results of the iron/oxygen reconstitution reaction were that the tryptophan mutant formed a transient neutral tryptophan radical ($W^{\bullet}$) visible for a few minutes at room temperature. This radical was, however, not able to initiate RNR catalysis in the holoenzyme. In the cysteine and phenylalanine mutants, a paramagnetic intermediate called X, formally described as an Fe(III)/Fe(IV) state like in the corresponding reaction with native R2 proteins, was observed. Intermediate X in these mutants had a considerably longer lifetime than in the native mouse R2 protein. The X intermediate was not able to form any EPR-observable successor radicals in the cysteine or phenylalanine mutants.

In the present work, a double mutant of the mouse R2 protein was constructed. The radical-harboring Tyr^{177} was engineered to hinder radical formation at that residue to a phenylalanine, and at the same time, Ile^{263} was replaced by a cysteine (Figure 1). This mutation places the cysteine residue at the same distance from the iron center as Tyr^{177} and could perhaps give rise to a free radical associated with cysteine. The double mutant will hereafter be referred to as Y177F/I263C. We have used 9.6 and 285 GHz EPR spectroscopy to study the iron/oxygen reconstitution reaction in this mouse R2 double mutant. The ultimate objective was to investigate the possibility of forming and observing a thiyl radical ($S^{\bullet}$) on cysteine. A thiyl radical has been proposed as the ultimate radical initiator in the substrate reaction in protein R1 (*3*). This type of radical is, however, extremely elusive and has never been directly observed as an endpoint in the radical transfer chain of RNR. The strategy here was to try to induce the thiyl radical directly in the vicinity of the iron site.

EXPERIMENTAL PROCEDURES

Expression and Purification of R2 Proteins. Construction of plasmids for overexpression of recombinant native mouse R2 protein has been described previously (*21*). The mouse R2 protein containing the double-mutation Y177F/I263C was expressed in *E. coli* using the pET expression system as

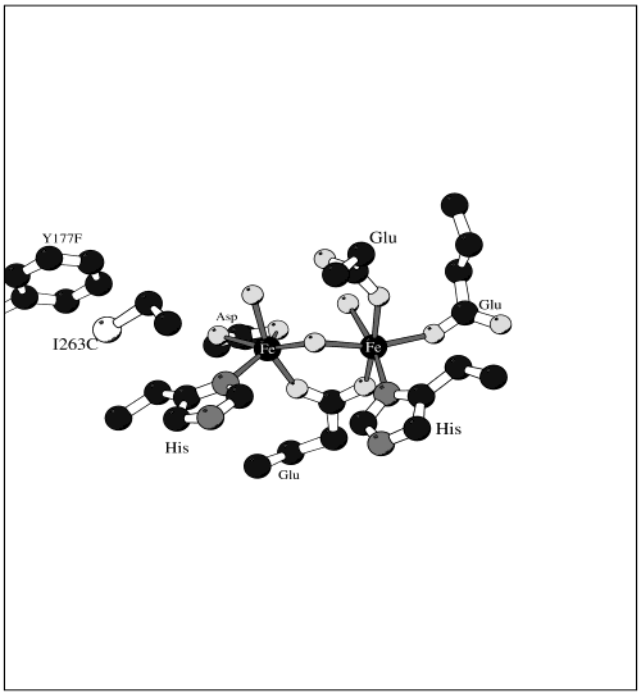

FIGURE 1: Model of the double mutant constructed from the *E. coli* R2 iron center superpositioned onto the mouse R2 structure. Cys263 is located about 6 Å from Fe1. The figure was made using Molscript (46). Atoms are colored as follows: black, carbon; dark gray, nitrogen; light gray, oxygen (except I263C, sulfur).

described earlier (*12*). In the mutagenesis, we started with the pET R2Y177F plasmid (*18*). The I263C mutation was introduced using the QuikChange Site-Directed Mutagenesis Kit (Stratagene) and the oligonucleotides 5′ GAG CTT **TGT** AGC AGA GAC 3′ and 5′ TCT GCT **ACA** AAG CTC ATT 3′. After verifying the correct DNA sequence by dideoxyribonucleotide sequencing, the pET R2 Y177FI263C vector was transfected into *E. coli* Bl21(DE3)pLysS bacteria.

Recombinant native mouse R2 protein was overexpressed as previously described (*21*). Mutant protein was overexpressed as described in (*14*).

Frozen bacteria were gently thawed in a 25 °C water bath and centrifuged at 45 000 rpm for 45 min at 4 °C. Purification procedures for native and mutant R2 proteins were performed as previously described for native R2 protein (*21*). The mutant protein was in the apo form (metal-free) after purification.

Protein purity was analyzed by SDS-polyacrylamide gel electrophoresis. The protein R2 concentrations were determined from the absorbance at 280 nm minus the absorbance at 310 nm ($E_{280-310} = 124\,000\ M^{-1}\ cm^{-1}$) using a Varian Cary-4 spectrophotometer.

Assay of Ribonucleotide Reductase Activity. The activity of mouse R2 Y177F/I263C protein was determined in the presence of an excess of recombinant R1 protein (*22*) as described earlier (*14*).

Preparation of the Anaerobic Fe^{2+} Solution. Buffer containing 50 mM Tris/HCl 100 mM KCl, pH 7.6, was thoroughly degassed in a septum-sealed bulb for several hours by repeatedly flushing with oxygen-free argon and evacuation. A second bulb containing Mohr's salt crystals $(NH_4)_2Fe(SO_4)_2$ was sealed with a septum and degassed according to the same procedure. The bulbs were then left under a slight excess pressure of argon. A plastic syringe

was made anaerobic by washing several times with oxygen-free argon gas. Then the appropriate volume of anaerobic buffer to prepare the desired iron concentration was transferred into the bulb containing Mohr's salt.

Reconstitution Reaction of Protein R2 with Fe^{2+} and Oxygen. Reconstitution of the iron site in the R2 proteins were carried out by mixing equal volumes of protein in oxygen-saturated 50 mM Tris/HCl 100 mM KCl, pH 7.6, with a ratio of anaerobic Fe^{2+} solution to protein R2 dimer of 6:1.

Rapid Freeze Quenching (RFQ). RFQ was performed with a System 1000 apparatus from Update Instruments to obtain reaction times from 8 ms to 1 s. The reaction times were varied by changing the length of the reaction tube between mixer and spray nozzle. An EPR tube connected with a funnel fixed in a home-built holder was immersed completely into an isopentane bath between −110 and −120 °C. Aerobic apoprotein and anaerobic Fe^{2+} solution were rapidly mixed and then quenched by spraying them into the EPR tube in the isopentane bath. The crystals were tightly packed into the EPR tube using a packing rod made from Teflon. The isopentane in the EPR tube was removed, and then the EPR tubes were kept for at least 20 min under high vacuum to get rid of isopentane trapped between the crystals. During this time, the tubes were stored in a separate *n*-pentane bath of −120 °C.

Slow Freeze Quenching (SFQ). For reaction times spanning between 3 and 1200 s, SFQ samples were obtained by hand-mixing. EPR tubes with the aerobic protein solution and a septum-sealed bulb with the anaerobic Fe^{2+} solution were thermostated at the reaction temperature in a water bath. A gastight Hamilton syringe, equipped with a long needle, was washed several times with the anaerobic Fe^{2+} solution to remove oxygen. Then the anaerobic ferrous solution was mixed with the apoprotein and the reaction stopped by immersing the EPR tube into cold *n*-pentane (−120 °C).

For reaction times longer than 1200 s, samples were produced by thawing SFQ samples with shorter reaction times, letting the reconstitution reaction proceed for a certain time (at a controlled reaction temperature), and then refreezing the samples by immersing the EPR tubes into cold *n*-pentane (−120 °C).

EPR Measurements: 9.6 GHz EPR. Spectra were recorded on a Bruker Elexsys E500 system using a rectangular dual-mode Bruker EPR cavity (ER 4116DM). For measurements below 77 K, the spectrometer was equipped with an Oxford helium flow cryostat. Spin quantitation was performed using a Cu^{2+}/EDTA (1 mM/10 mM) primary standard or by a sample of native mouse R2 with a known tyrosyl radical content by comparing the double integrals under nonmicrowave saturating conditions. Spectra were evaluated using Xepr 2.0 software from Bruker.

285 GHz EPR. Spectra were recorded at 5 K in the Grenoble High Magnetic Field Laboratory (CNRS-MPI, Grenoble, France) as previously described (*23*). The frequency source used to generate a 285 GHz excitation is a Gunn-diode delivering a 95 GHz basic frequency, which is then tripled to obtain 285 GHz (system supplied by Radiometer Physics GmbH). The basic frequency can be changed ±50 MHz. The exact frequency used was recorded automatically by the system.

Scheme 1

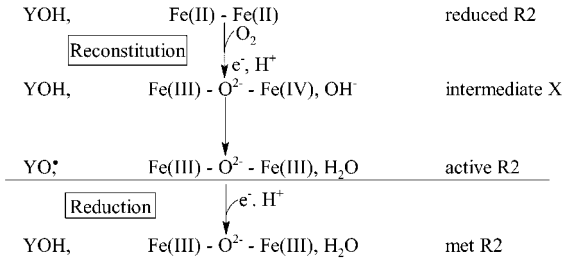

EPR powder spectra were simulated (anisotropic *g*-values and hyperfine tensors) using the program WinEPR Simfonia 1.25 from Bruker.

Structure Modeling of the Y177F/I263C Double Mutant of Mouse R2. The only three-dimensional structure of mouse protein R2 determined so far was obtained at a low pH and showed only one iron atom in the dinuclear center (*11*). Therefore, a model of a dinuclear iron center in mouse protein R2 was constructed by superpositioning the *E. coli* R2 structure (*7*,*8*) onto mouse R2, using the iron positions and ligands from *E. coli* R2 but keeping the rest of the mouse R2 structure (*11*). The Y177F and I263C mutations were made using the computer program O (*24*). The F177 side chain was positioned with the same conformation as the native Tyr, and the Cys side chain was modeled in the most common rotamer. This procedure positions the S_γ atom of Cys close to the corresponding C_γ atom of the native Ile.

RESULTS

The reconstitution reaction of *E. coli* protein R2, where the reduced iron site reacts with molecular oxygen and the tyrosyl radical is formed, is briefly described in Scheme 1. When oxygen becomes bound, the reaction is proposed to proceed via a number of intermediates, of which the so-called intermediate X is the only relatively well-characterized one. It is formally described as a paramagnetic $Fe^{III}-Fe^{IV}$ center with an iron−iron distance of about 2.5 Å. It is considered to be the precursor to the tyrosyl radical (*15*, *25*−*29*). The scheme also defines the met form of R2, where the tyrosyl radical has been reduced but the diferric center is intact.

In the native mouse R2 protein, the reconstitution is proposed to follow a similar pathway (*15*). The different kinetic conditions, however, make intermediate X much more short-lived in the native mouse protein, and it is not generally observed in the reconstitution reaction under the conditions employed here (*15*). Intermediate X is, however, quite long-lived in the mouse R2 mutants Y177F and Y177C, where no successor radical is formed (*18*). In a recent report (*30*) where somewhat different conditions were used for the reconstitution reaction, intermediate X could be clearly observed also in native mouse R2.

Enzyme Activity. No significant activity could be demonstrated for the Y177F/I263C R2 protein assayed in the presence of an excess of mouse R1 protein (data not shown).

Light Absorption Spectroscopy. Mutant apoprotein R2 Y177F/I263C was reconstituted with Fe^{2+} (6 Fe^{2+}/R2 dimer) and molecular oxygen. The light absorbance after reconstitution significantly increased in the 300−400 nm region. However, the two partly resolved absorption bands characteristic for a μ-oxo-bridged diferric iron center at 320 and 370 nm were not resolved (data not shown). The met form

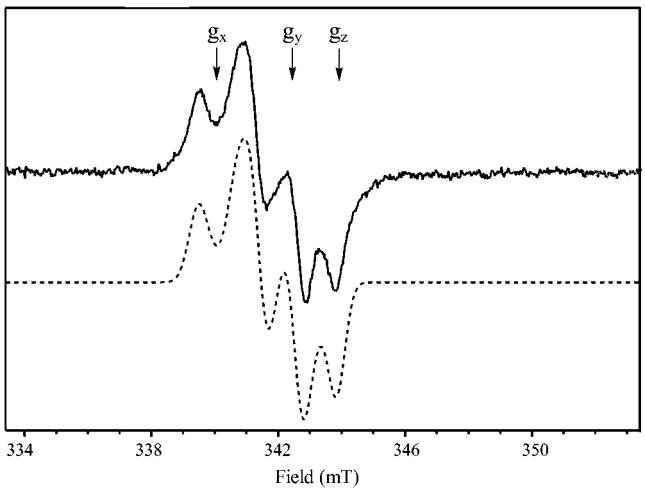

FIGURE 2: EPR spectra of the sulfinyl radical from mouse R2 Y177F/I263C (solid line) and the simulated spectrum (broken line). The reconstitution reaction was quenched after 60 s at 5 °C. Recording conditions: frequency 9.6 GHz, temperature 20 K, field modulation 5 G, microwave power 0.5 milliwatts. The *g*-tensor components g_x, g_y, and g_z for the sulfinyl radical are indicated by arrows.

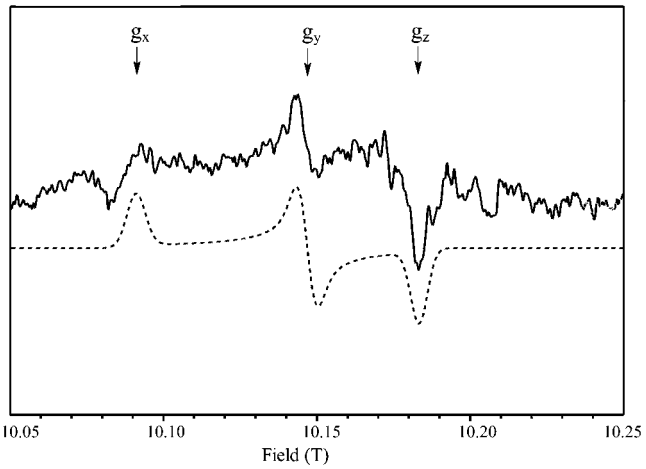

FIGURE 3: EPR spectra at 285 GHz of the sulfinyl radical from 0.3 mM R2 Y177F/I263C (solid line) reconstituted with 6 Fe/R2 at 5 °C and the simulated spectrum (broken line). The reaction was quenched after 40 s. Recording conditions: frequency 285 GHz, temperature 5 K, field modulation 25.5 mA. The *g*-tensor components g_x, g_y, and g_z for the sulfinyl radical are indicated by arrows. The simulated contribution of Mn^{2+} has been subtracted from the experimental curve.

Table 1. Comparison of Radical *g*-Anisotropy in Different Organic Compounds and Proteins

compound	g_x	g_y	g_z	Δg $(g_x - g_z)$	ref
methyl mercaptan	2.020	2.0094	2.0021	0.0179	48
tert-butyl mercaptan	2.0201	2.0095	2.0025	0.0176	48
n-butyl mercaptan	2.021	2.011	2.0032	0.0178	48
cysteamine	2.0209	2.0093	2.0027	0.0182	48
PFL mutant	2.0204	2.0084	2.0005	0.0199	33
Y177F/I263C (RNR mouse R2)	2.0206	2.0093	2.0022	0.0184	this work
$Y^{\bullet}$ (RNR mouse R2)	2.0076	2.0043	2.0022	0.0054	49
$Y^{\bullet}$ (RNR *E. coli* R2)	2.0086	2.0042	2.002	0.0066	50
$Y^{\bullet}_D$ (PSII)	2.0075	2.0042	2.0022	0.00523	51

Table 2. Quantitation of the Sulfinyl Radical Obtained in the Reconstitution Reaction of Mouse ApoR2 Y177F/I263C and Ferrous Iron in the Presence of O_2[a]

reaction time (s)	unpaired spins/R2	reaction time (s)	unpaired spins/R2
5	0.06	720	0.3
10	0.07	960	0.3
20	0.1	1200	0.2
40	0.1	1800	0.2
60	0.2	2400	0.2
240	0.3	3600	0.2
480	0.2	7200	0.1

[a] All experiments were done in 50 mM Tris/HCl 100 mM KCl, pH 7.6, with a ratio of ferrous iron to protein R2 dimer of 6. The reaction temperature was 5 °C.

of native mouse protein R2 (*21*, *31*) and some mouse mutants show similar badly resolved light absorption spectra in the iron absorption region as seen for this double mutant (*12*, *18*).

EPR Spectroscopy. Mutant apoprotein R2 Y177F/I263C was reconstituted with Fe^{2+} (6 Fe^{2+}/R2 dimer) and molecular oxygen. By combining RFQ and SFQ methods, the reaction was followed from 8 ms to 120 min. EPR spectroscopy was used to detect any paramagnetic intermediates appearing in the reaction.

Figure 2 shows the 9.6 GHz EPR spectra of the radical signal when the reconstitution reaction was quenched after 60 s of reaction time at 5 °C. Computer simulation of the spectrum allowed evaluation of *g*-values and hyperfine couplings. The simulation parameters for the radical were $g_x = 2.0206$, $g_y = 2.0093$, $g_z = 2.0022$, and $A_{iso} = 1.24$ mT, which gives a *g*-anisotropy value, $\Delta g = g_x - g_z$, of 0.0184. These values are very close to the ones reported in the literature for frozen solution spectra of sulfinyl radicals formed from cysteine or sulfhydryl molecules, as summarized in Table 1.

High-field EPR at 285 GHz, corresponding to a magnetic field of about 10.1 T, was used to further characterize the radical signal. Figure 3 shows the high-field spectrum of the radical after 40 s of reaction time at 5 °C. A computer simulation in good agreement with experimental observations was obtained by using the *g*-anisotropy value evaluated at 9.6 GHz. This confirms the *g*-value anisotropy evaluated from the results at 9.6 GHz, and we hereby assign the signal to a sulfinyl radical ($SO^{\bullet}$).

The total amount of unpaired spins observed per R2 is summarized in Table 2. It shows that a maximum of about 0.2−0.3 sulfinyl radical/R2 is observed after 4 min of reaction time. This amount remains relatively stable for at least 2 h at 5 °C, after which the protein itself starts to precipitate. We will therefore consider the sulfinyl radical to be stable on the hour time scale.

The microwave relaxation behavior at 9.6 GHz EPR of the sulfinyl radical at different temperatures is presented in Figure 4. Table 3 summarizes the EPR relaxation parameters of the sulfinyl radical at different temperatures. A comparison with the tyrosyl radical from native mouse R2 is also made. The table gives the parameters in terms of microwave power at half-saturation $P_{1/2}$ and *b*. The parameter *b* describes the contribution of inhomogeneous broadening (*32*) to the saturation curve as shown in eq 1,

$$I \propto 1/(1 + P/P_{1/2})^{b/2} \quad (1)$$

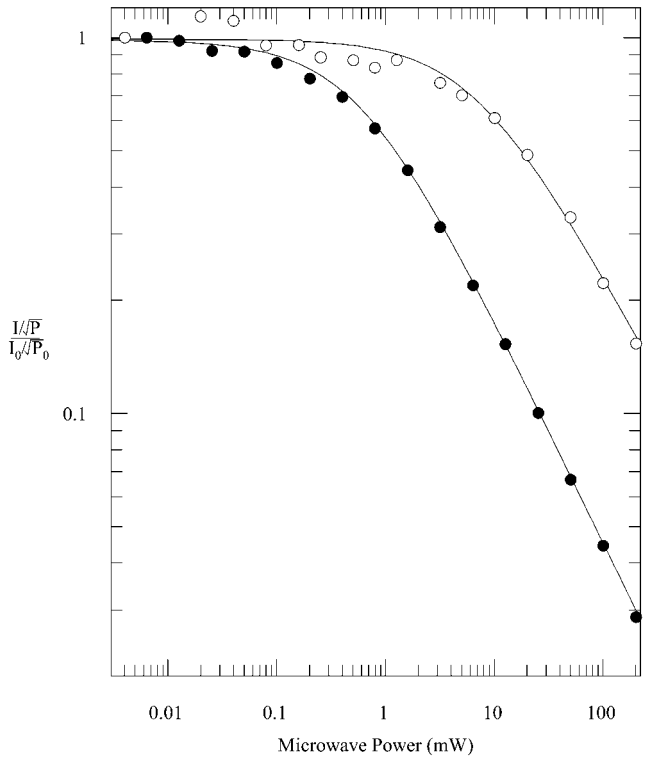

FIGURE 4: EPR microwave power saturation curves of the sulfinyl radical from mouse R2 Y177F/I263C in the temperature range 20−30 K. The reconstitution reaction was quenched after 60 s at 5 °C. Continuous traces are computer fits as described in the text: 20 K (●); 30 K (○).

Table 3. Comparison of $P_{1/2}$[a] Values of R2 Tyrosyl Radicals from *E. coli*, *M. tuberculosis*, and Mouse and the Sulfinyl Radical from Mouse Y177F/I263C R2

		$P_{1/2}$ (mW)			
radical	source	20 K	30 K	R^b	ref
Tyr•	*Mtb* R2-2	0.25	0.31	1.2	52
Tyr•	*E. coli* R2	0.024	0.078	3.3	16
Tyr•	mouse R2[c,d]	0.53	9.85	18.6	this work
SO•	mouse Y177F/I263C R2[c,e]	0.58	6.86	11.8	this work

[a] $P_{1/2}$ values were estimated from a computer fit of microwave saturation curves (eq 1). [b] $R = P_{1/2}(30\text{ K})/P_{1/2}(20\text{ K})$. [c] Values of *b* were estimated from a computer fit of microwave saturation curves (eq 1). [d] Values of *b* were 1.17 and 1.47 at 20 and 30 K, respectively. [e] Values of *b* were 1.19 and 1.07 at 20 and 30 K, respectively.

where *I* is EPR amplitude and *P* is the microwave power. The relaxation properties of the sulfinyl radical are quite similar to those of the native tyrosyl radical in mouse R2, confirming that the sulfinyl radical in mouse Y177F/I263C is located relative to the iron center in a way similar to the tyrosyl radical in native mouse R2.

In an attempt to characterize any early appearing paramagnetic intermediates in the formation of the sulfinyl radical, a rapid freeze quench technique was used to follow the reconstitution reaction. This technique enables the production of samples with reaction times as short as 8 ms. Figure 5 shows a series of EPR spectra obtained after reaction times spanning between 20 ms and 20 s. The weak signals observed at early reaction times (between 20 and 500 ms) exhibit axial symmetry, with a $g_{||}$ and $g_{\perp}$ component as indicated in the figure. The sulfinyl signal observed after 20 s has rhombic symmetry with three principal *g*-components,

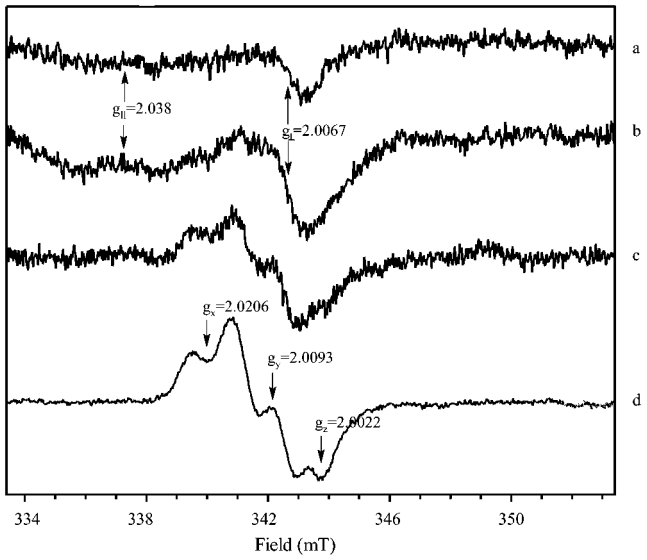

FIGURE 5: EPR spectra of mouse apoR2 Y177F/I263C reconstituted with 6 Fe^{2+}/R2 freeze quenched after varying reaction times: (a) 20 ms, (b) 500 ms, (c) 5 s, and (d) 20 s. Reaction temperatures were 22 °C (a and b) and 5 °C (c and d). Recording conditions: frequency 9.6 GHz, temperature 20 K, field modulation 10 G, microwave power 0.5 milliwatts.

g_x, g_y, and g_z. The EPR signals between 500 ms and 5 s can be explained as mixtures of the two components. The apparent *g*-values of 2.038 and 2.0067 observed for the axial signals are compatible with those reported in the literature for peroxyl radicals ($g_{||} = 2.034$, $g_{\perp} = 2.007$) (*33*). No obvious EPR signal that could be ascribed to intermediate X was observed.

DISCUSSION

In native mouse R2, the protein-linked stable tyrosyl free radical located at Y177 is observed upon reconstitution with ferrous iron and molecular oxygen (Scheme 1). One stabilizing factor of this tyrosyl radical has been proposed to be a hydrophobic pocket in close vicinity of the radical site. The pocket in native mouse R2 is composed of three conserved hydrophobic residues, F237-F241-I263C (*7*, *11*).

In this study, we have observed a new stable sulfinyl radical in mouse protein R2 upon reconstitution of the double-mutant R2-Y177F/I263C. The assignment of the observed signal is based on *g*-anisotropy values, compatible with what has previously been reported in the literature for sulfinyl radicals, obtained from 9.6 GHz EPR studies of the reconstitution reaction (Figure 2 and Table 1). Additional 285 GHz EPR confirmed the assignment (Figure 3). A maximum of 0.2−0.3 sulfinyl radical/R2 was observed after 4 min of reaction time at 5 °C, and this radical content remained relatively constant over the lifetime of the protein (about 2 h at the reaction temperature), as summarized in Table 2. This yield is smaller than that of the tyrosyl radical in native mouse R2, which has been reported as high as 1.6/R2 (*34*). The time scale for sulfinyl radical formation is slower than that of the tyrosyl radical in native mouse under similar conditions (*15*). The increase of the light absorption band between 300 and 400 nm during the reconstitution reaction suggests that a seemingly normal diiron cluster is formed.

It is already known from earlier studies that protein R2 with the single mutation Y177F is not capable of forming

any successor radical despite the observations of a relatively long-lived intermediate X (*18*). We therefore consider the observed sulfinyl radical to be a result of the additional mutation introduced at position 263, where isoleucine is replaced by a cysteine amino acid (Figure 1). The sulfinyl radical should be situated on C263, and the surroundings of this residue may explain the unusual radical stability. The two remaining residues of the hydrophobic pocket, F237 and F241, are still intact, and an additional phenylalanine, F177, introduced by mutation of Y177, is now also in very close vicinity of C263. All together, they are expected to create a protecting environment for the sulfinyl radical, much like the hydrophobic pocket in the native R2 protein.

The EPR relaxation properties for the tyrosyl radical in a native R2 protein reflect the influence of the neighboring iron site, which is antiferromagnetically coupled (*35*). The estimated values of microwave power at half saturation ($P_{1/2}$, eq 1) and its temperature dependence vary between tyrosyl radicals in R2 proteins from different species in comparison with the results obtained for native mouse R2 and the double-mutant Y177F/I263C observed here (Table 3). The species-dependent variations reflect the different environments of the tyrosyl radicals and, in particular, the interaction with the iron sites. The high values of $P_{1/2}$ for native mouse R2, particularly at higher temperatures, have been interpreted as a strong coupling between the radical and the iron site, in contrast to the situation in wild-type *E. coli* and *Mycobacterium tuberculosis* R2. The sulfinyl radical from Y177F/I263C has relaxation properties similar to those of the tyrosyl radical in native mouse R2, indicating that the radicals interact with the iron sites in similar ways. This strongly supports the localization of the sulfinyl radical to C263, which is located at a distance from the iron site similar to that of Y177 in the native protein (Figure 1).

Pyruvate formate-lyase (PFL) plays a central role in the metabolic pathway of glucose in *E. coli* and is a prototype of the family of *S*-adenosyl-methionine-dependent glycyl radical-containing enzymes, including the class III RNR (*36*). Under strictly anaerobic conditions, active PFL contains a relatively stable glycyl radical, essential for catalytic activity (*37*−*39*). In contrast to many other radical-containing enzymes such as the class I RNR, the radical residue in this family is situated close to the active site. Thus, the radical does not have to undergo long-range transfer from the glycyl residue to the active site for catalysis. Site-directed mutagenesis studies have shown that two cysteines, C418 and C419, are also essential for catalysis, but not required for generation and stabilization of the glycyl radical (*40*, *41*). The catalytically active agent is probably a cysteinyl radical on C419, formed concomitantly with the substrate binding. This situation with radical transfer from one residue to another for catalysis is similar to that proposed for class I RNR. Active PFL is rapidly inactivated by exposure to oxygen, and this reaction has been used to define the site of the stable radical in the active enzyme as glycine 734 (G734) (*42*, *43*). In an EPR investigation of the oxygen inactivation mechanism in wild-type PFL and mutant PFL enzymes, in which either or both of C418 and C419 were replaced by an alanine, formation of two protein-based radical intermediates was observed. A long-lived sulfinyl radical (C−SO•) located at C419 was obtained in the wild-type protein and in the C418A mutant. A peroxyl radical (RSOO•) at G734 was observed in the C419A and C418A/C419A mutants and transiently in wild-type PFL (*33*). A mechanism describing the formation of the radical intermediates was proposed, and its feasibility was later tested in theoretical calculations (*44*). A recent study of wild-type and mutant PFLs, using RFQ EPR, further supports the earlier findings. The proposed detailed mechanism suggests that molecular oxygen reacts with the glycyl radical in the active enzyme. The resulting peroxyl radical on glycine reacts further with the sulfhydryl group of the 419 residue to form the long-lived sulfinyl radical (*45*).

The RFQ EPR spectra observed here in the reconstitution reaction of the mouse R2 double-mutant Y177F/I263C (Figure 5) exhibit a pattern similar to that in PFL: early formation of a transient radical that may be assigned to a peroxyl radical, followed by a stable (in our case) sulfinyl radical, probably on C263. We have not been able to establish any detailed kinetic relationship between the two types of radicals in the Y177F/I263C R2 mutant. Furthermore, it is not immediately possible to assign the proposed peroxy radicals to a particular residue type, since peroxy radicals give very similar EPR spectra for several different amino acid side chains (*46*). The role of the proposed peroxy radicals as precursors to the sulfinyl radicals in the present case is therefore not proven. However, if one assumes that a reaction pathway similar to that in native R2 operates in the R2 mutant, then the "normal" reconstitution reaction should continue until the formation of intermediate X. Then C263 would give rise to a cysteinyl radical RS•. A second O_2 could react with RS• to give RSOO•, which would undergo reductive cleavage to form RSO• and water.

The experiments reported here on the mouse R2 double-mutant Y177F/I263C show the generality of the radical formation in the reaction where the diiron center is formed in the Fe^{2+}/O_2 reconstitution reaction in protein R2. The functional significance of the observed sulfinyl radicals is that we have for the first time stabilized a well-defined and site-specific cysteine-based free radical in ribonucleotide reductase, albeit far from the active site in the R1 protein. In the vicinity of the iron site in protein R2, it is clearly possible to produce and in some mutant cases stabilize various amino acid side-chain radicals. The native R2 proteins have probably evolved so as not to have ionizable residues in the vicinity, apart from the native tyrosyl residue. We also find a relationship between mutants of RNR and PFL, in that mutated forms of both types of enzymes can harbor relatively stable SO• radicals.

ACKNOWLEDGMENT

We thank H. Eklund, Department of Molecular Biology, Swedish University of Agricultural Sciences, Uppsala, for performing the modeling of Y177F/I263C and T. Astlind, Department of Biochemistry and Biophysics, Stockholm University, for technical support.

REFERENCES

1. Reichard, P. (1993) *Science 260*, 1773−1777.
2. Sjöberg, B.-M. (1995) in *Nucleic Acids and Molecular Biology* (Eckstein, F., and Lilley, D. M. J., Eds.) Vol. 9, pp 192−221, Springer-Verlag, Berlin.
3. Sahlin, M., and Sjöberg, B.-M. (2000) in *Subcellular Biochemistry* (Holzenburg and Scrutton, Eds.) Vol. 35, pp 405−443, Kluwer Academic/Plenum Publishers, New York.

4. Larsson, Å., and Sjöberg, B.-M. (1986) *EMBO J. 5*, 2037−2040.
5. Sjöberg, B.-M. (1997) *Struct. Bond. 88*, 139−173.
6. Stubbe, J., and van der Donk, W. A. (1998) *Chem. Rev. 98*, 705−762.
7. Nordlund, P., Sjöberg, B.-M., and Eklund, H. (1990) *Nature 345*, 593−598.
8. Nordlund, P., and Eklund, H. (1993) *J. Mol. Biol. 232*, 123−164.
9. Uhlin, U., and Eklund, H. (1994) *Nature 370*, 533−539.
10. Thelander, L., and Gräslund, A. (1994) in *Metal Ions in Biological Systems* (Sigel, H., and Sigel, A., Eds.) Vol. 30, Chapter 4, pp 109−129, Marcel Dekker, Inc., New York.
11. Kauppi, B., Nielsen, B. B., Ramaswamy, S., Kjøller-Larsen, I., Thelander, M., Thelander, L., and Eklund, H. (1996) *J. Mol. Biol. 262*, 706−720.
12. Rova, U., Goodtzova, K., Ingemarson, R., Behravan, G., Gräslund, A., and Thelander, L. (1995) *Biochemistry 34*, 4267−4275.
13. Ekberg, M., Sahlin, M., Eriksson, M., and Sjöberg, B.-M. (1996) *J. Biol. Chem. 271*, 20655−20659.
14. Rova, U., Adrait, A., Pötsch, S., Gräslund, A., and Thelander, L. (1999) *J. Biol. Chem. 274*, 23746−23751.
15. Schmidt, P. P., Rova, U., Katterle, B., Thelander, L., and Gräslund, A. (1998) *J. Biol. Chem. 273*, 21463-21472.
16. Sahlin, M., Petersson, L., Gräslund, A., Ehrenberg, A., Sjöberg, B.-M., and Thelander, L. (1987) *Biochemistry 26*, 5541−5548.
17. Ormö, M., Regnström, K., Wang, Z., Que, L., Sahlin, M., and Sjöberg, B.-M. (1995) *J. Biol. Chem. 270*, 6570−6576.
18. Pötsch, S., Lendzian, F., Ingemarsson, R., Hörnberg, A., Thelander, L., Lubitz, W., Lassmann, G., and Gräslund, A. (1999) *J. Biol. Chem. 274*, 17696−17704.
19. Sahlin, M., Lassmann, G., Pötsch, S., Sjöberg, B.-M., and Gräslund, A. (1995) *J. Biol. Chem. 270*, 12361−12372.
20. Lendzian, F., Sahlin, M., MacMillan, F., Bittl, R., Fiege, R., Pötsch, S., Sjöberg, B.-M., Gräslund, A., Lubitz, W., and Lassmann, G. (1996) *J. Am. Chem. Soc. 118*, 8111−8120.
21. Mann, G. J., Gräslund, A., Ochiai, E.-I., Ingemarson, R., and Thelander, L. (1991) *Biochemistry 30*, 1939−1947.
22. Davis, R., Thelander, M., Mann, G. J., Behravan, G., Soucy, F., Beaulieu, P., Lavalleé, P., Gräslund, A., and Thelander, L. (1994) *J. Biol. Chem. 269*, 23171−23176.
23. Barra, A.-L., Brunel, L. C., and Robert, J. B. (1990) *Chem. Phys. Lett. 165*, 107−109.
24. Jones, T. A., Zou, T. Y., Cowan, S. W., and Kjeldgaard, M. (1991) *Acta Crystallogr. 47*, 110−119.
25. Sturgeon, B. E., Burdi, D., Chen, S., Huynh, B. H., Edmondson, D. E., Stubbe, J., and Hoffman, B. M. (1996) *J. Am. Chem. Soc. 118*, 7551−7557.
26. Willems, J. P., Lee, H. I., Burdi, D., Doan, P. E., Stubbe, J., and Hoffman, B. M. (1997) *J. Am. Chem. Soc. 119*, 9816−9824.
27. Ling, J. S., Sahlin, M., Sjöberg, B.-M., Loehr, T. M., and Sanders-Loehr, J. (1994) *J. Biol. Chem. 269*, 5595−5601.
28. Que, L., and Stubbe, J. (1998) *J. Am. Chem. Soc. 120*, 849−860.
29. Bollinger, J. M., Edmondson, D. E., Huynh, B. H., Filley, J., Norton, J. R., and Stubbe, J. (1991) *Science 253*, 292−298.
30. Yun, D., Krebs, C., Gupta, G., Iwig, D., Huynh, B., and Bollinger, M., Jr. (2002) *Biochemistry 41*, 981−990.
31. Davydov, A., Schmidt, P. P., and Gräslund, A. (1996) *Biophys. Biochem. Res. Commun. 219*, 213−218.
32. Sahlin, M., Gräslund, A., and Ehrenberg, A. (1986) *J. Magn. Reson. 67*, 135−137.
33. Reddy, S. G., Wong, K. K., Parast, C. V., Peisach, J., Magliozzo, R. S., and Kozarich, J. W. (1998) *Biochemistry 37*, 558−563.
34. Ochiai, E. I., Mann, G. J., Gräslund, A., and Thelander, L. (1990) *J. Biol. Chem. 256*, 15758−15761.
35. Petersson, L., Gräslund, A., Sjöberg, B.-M., Reichard, P., and Ehrenberg, A. (1980) *J. Biol. Chem. 255*, 6706−6712.
36. Knappe, J., Blaschkowski, H. P., Grobner, P., and Schmitt, T. (1974) *Eur. J. Biochem. 50*, 253−263.
37. Knappe, J., Neugebauer, F. A., Blaschkowski, H. P., and Ganzler, M. (1984) *Proc. Natl. Acad. Sci. U.S.A. 81*, 1332−1335.
38. Unkrig, V., Neugebauer, F. A., and Knappe, J. (1989) *Eur. J. Biochem. 184*, 723−728.
39. Wagner, A. F. V., Frey, M., Neugebauer, F. A., Schafer, W., and Knappe, J. (1992) *Proc. Natl. Acad. Sci. U.S.A. 89*, 996−1000.
40. Knappe, J., Albert, S., Frey., M., and Wagner, A. F. V. (1993) *Biochem. Soc. Trans. 21*, 731−734.
41. Prast, C. V., Wong, K. K., Kozarich, J. W., Peisach, J., and Magliozzo, R. S. (1995) *Biochemistry 34*, 2393−2399.
42. Leppanen, V.-M., Merckel, M. C., Ollis, D. L., Wonf, K. K., Kozarich, J. W., and Goldman, A. (1999) *Structure 7*, 733−744.
43. Becker, A., Fritz-Wolf, K., Kabsch, W., Knappe, J., Schultz, S., and Wagner, A. F. V. (1999) *Nat. Struct. Biol. 6*, 969−975.
44. Gauld, J. W., and Eriksson, L. A. (2000) *J. Am. Chem. Soc. 122*, 2035−2040.
45. Zhang, W., Wong, K. K., Magliozzo, R. S., and Kozarich, J. W. (2001) *Biochemistry 40*, 4123−4130.
46. Sahlin, M., Cho, K.-B., Pötsch, S., Lytton, S., Huque, Y., Gunther, M., Sjöberg, B.-M., Mason, R. P., and Gräslund, A. (2002) *J. Biol. Inorg. Chem. 7*, 74−82.
47. Kraulis, P. (1991) *J. Appl. Crystallogr. 24*, 946−950.
48. Swarts, S. G., Becker, D., DeBolt, S., and Sevilla, M. D. (1989) *J. Phys. Chem. 93*, 155−161.
49. Schmidt, P. P., Andersson, K. K., Barra, A.-L., Thelander, L., and Gräslund, A. (1996) *J. Biol. Chem. 271*, 23615−23618.
50. Un, S., Atta, M., Fontecave, M., and Rutherford, A. W. (1995) *J. Am. Chem. Soc. 117*, 10713−10719.
51. Un, S., Tang, X.-S., Diner, B. A. (1996) *Biochemistry 35*, 679−684.
52. Liu, A., Pötsch, S., Davydov, A., Barra, A.-L., Rubin, H., and Gräslund, A. (1998) *Biochemistry 37*, 16369−16377.

BI012043D